Proceedings of the Canadian Society for Mechanical Engineering International Congress
32nd Annual Conference of the Computational Fluid Dynamics Society of Canada
Canadian Society of Rheology Symposium
CSME/CFDSC/CSR 2025
May 25–28, 2025, Montréal, Québec, Canada

NUMBER

EVALUATION OF BRAKING STRATEGIES FOR COLLISION AVOIDANCE

Robert Boccanfuso[1], B. Minaker[2],

[1]MAME, University of Windsor, Windsor, Canada

Jan 29, 2025

***Abstract*—**While the concept of automated highway driving seems trivial at first, there are many hazards scattered throughout a constantly changing environment. Many of the proposed driving strategies however, are often limited to control well within vehicle limits. It is due to the complexity of developing robust control around these limits that fully autonomous vehicles remain a figment of the future. To assist this area of research, a study was conducted to test the effectiveness of different braking strategies during a collision avoidance scenario. Across studies, braking strength and distance were varied to evaluate handling performance at different operating points around the vehicle limits. Upon analysis of the collected data, it was discovered that the addition of braking can increase the effectiveness of the maneuver when employed correctly. Additionally, it was found that the braking strength of the vehicle played a significantly larger role in the maneuver's effectiveness than braking distance. Although results were only plotted for a few points around the vehicle's traction circle, the results demonstrated trends which could be extrapolated to predict the vehicle's performance at other operating points.

***Keywords-component*—autonomous vehicles; vehicle dynamics; collision avoidance;**

I. INTRODUCTION

While the concept of automated highway driving seems trivial at first, there are many hazards scattered throughout a constantly changing environment. The nature of these hazards range greatly from stationary objects such as construction barriers and lane closures to dynamic and unpredictable drivers. With the rapid push for development of automated driving technology, there is an abundance of research focused on the development of path-planning strategies. Many of these strategies however, prioritize occupant safety and comfort well within the limits of vehicle performance. While this is no issue under typical conditions, many driver assistance systems require the driver to maintain supervision and take over when vehicle control is critical. Often times, these scenarios are extremely time-sensitive and occur when a relatively aggressive maneuver is required to avoid an obstacle. In these scenarios, operating at or close to vehicle limits can be the difference between safety and catastrophe. To maximize the likelihood of collision avoidance in these scenarios, the full potential of the vehicle should be used. Because of the precise control required in these situations, it is of great interest to automate the process through robust control methods.

In racing, there is common reference to a term known as a tire's 'traction circle' [1]. As the tires are the only method of contact between the vehicle and the road, it is easy to see how maximizing tire output correlates to maximizing vehicle performance. Using a simple friction model, it can be shown that the maximum force a tire can output is a function of the normal force acting on it and the coefficient of friction between the tire and the road surface. Assuming no disturbances or changes in the coefficient of friction, the maximum force remains constant. As a tire can generate both lateral (cornering) and longitudinal (acceleration) forces, the maximum force output of the tire can be found in any direction (provided the combined magnitude of the vector is equal to the maximum tire force) [1].

Because maximum vehicle performance can be found anywhere around the limits of the tractive circle, there are infinitely many strategies that can be employed in an active-collision scenario. For example, one driver may choose to brake before turning to enable the vehicle to turn harder during the maneuver, while another driver may choose a mixed strategy. Although both drivers in this example are operating at the vehicle limits, the distance required to complete each

maneuver may vary. As this question is non-trivial, a study was conducted to simulate and analyze various driving strategies with the goal of finding an optimal point of operation.

II. METHODOLOGY

In order to study various control strategies in a meaningful fashion, a simulation was developed to analyze a lane-change maneuver. While travelling at highway speeds (in excess of 100 kph), the goal of the vehicle was to avoid an obstacle (leave its current lane) as quickly as possible. Across several simulations, braking time and strength were varied such that the vehicle was forced to operate at different locations around its tractive limits.

A. Model

Using the Equations of Motion (EoM) library for the Julia programming language [2] (a custom open-source software library which can compute the state-space and output matrices for a multi-body system), a multi-body vehicle model was generated. The model used was indicative of a generic front-wheel drive gasoline sedan with front MacPherson and rear quad-link suspensions. While the multi-body model described the state-space for the vehicle body and suspension dynamics, the tire forces were left as system inputs. The state-space was then imported into Simulink via a state-space block which was placed in a feedback loop with the PAC2002 tire mode [3]. Additional non-linear effects were also added to the system in a similar fashion.

In order to verify the developed model, a similar model was developed using Altair MotionView's Vehicle Wizard. As an initial comparison between the models, a linear eigenvalue analysis was conducted to evaluate similarities between suspension damping and stiffnesses. In addition to the frequency response of the model, some dynamic simulations were run to further evaluate the likeness of the models. Three experiments were conducted; a constant steer with increasing forward speed, a ramp steer under constant speed, and a sinusoidal steering profile at constant speed. Overall, a comparison of the obtained data demonstrated a good correlation between models. As a result of the agreement between models, the developed EoM model was found to be representative of a passenger vehicle.

B. Controller Design

In order to control the vehicle, controllers for both the steering and throttle inputs were required. Although simple in theory, accurate control of a vehicle can be very complex due to coupling between the longitudinal and lateral dynamics. In the field of controls, there are many types of controllers, each with their own benefits and drawbacks. Due to the precision of control required to operate at vehicle limits and the non-linearities present in the complex multi-body model, the choice of controller is critical.

1) Throttle Control: In 2021, a study performed by Samak et. al [4] attempted to evaluate various control strategies for autonomous vehicles. In the study, robust and predictable longitudinal control was achieved with a manually tuned PID controller. Therefore, PID control was chosen for the vehicle's throttle controller due to its simplicity.

2) Steering Control: While acceptable longitudinal control via PID can be achieved, the same study unfortunately found PID insufficient for lateral control. In the study, it was found that non-linear effects such as the coupling between the longitudinal and lateral dynamics resulted in unsatisfactory control. To accomplish more robust steering control, some researchers have turned towards more complex control methods such as model predictive control and neural networks [5][6][7]. In contrast to the more complicated strategies however, others have managed to achieve similar results through the development of a sliding mode controller [8][9]. As many iterations of various driving strategies were to be tested in this study, sliding mode control was chosen over other strategies due to its simplicity and ease of implementation.

Taking inspiration from [9], a sliding plane was developed to guide the vehicle through a lane-change maneuver. In the scenarios to be evaluated, the desired path of the vehicle would be affected by the error of the vehicle's location (y), and the vehicle's lateral speed in the global frame ($\dot{y}$). Based on these variables, a simple sliding surface was chosen:

$$s = y - k\dot{y} = 0 \tag{1}$$

Given:

$$\dot{y} = u\sin(\theta) \tag{2}$$

where:

- u is the vehicle's forward speed
- θ is the vehicle's heading angle
- k is a tuneable gain controlling the aggressiveness of the maneuver

Having chosen a linear sliding surface between the vehicle's displacement and its first derivative, the desired time-response of the system follows a smooth parabolic trajectory (see Figure 1). Although a lane change under normal conditions is typically approximated using a sine curve, it can be argued that a parabolic trajectory is more advantageous during an imminent collision scenario. At the beginning of the maneuver, while the obstacle is still approaching, the driver should attempt to avoid as quickly as possible. As it becomes clear that the obstacle will be avoided, the driver should become more concerned with reorienting the vehicle to prevent overshoot and remain inside the new lane.

In sliding mode control, the derivative of the sliding plane is zero as the system operates along it. By computing the derivative of the sliding plane, one can solve for the desired control. Under the assumption that the setpoint remains static throughout the maneuver, the equation can be solved for the desired yaw rate of the vehicle (r). Using the desired yaw rate

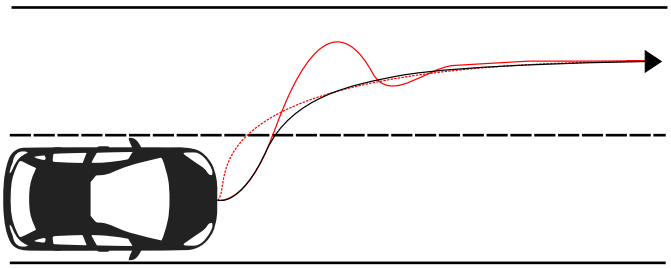

Figure. 1. Comparison between the vehicle's desired trajectory based on the SMC surface (red - dashed), the vehicle's actual trajectory, and a typical sinusoidal lane-change maneuver (black).

and forward speed of the vehicle, the required steering angle (δ) can then be computed:

$$\dot{s} = 0 = \dot{y} - k\ddot{y} \tag{3}$$

where $\dot{y}$ is defined by the sliding plane as:

$$\dot{y} = \frac{y}{k} = k_1 y \tag{4}$$

and $\ddot{y}$ can be solved for using chain rule on (2) assuming constant forward speed (u):

$$\ddot{y} = ur\cos(\theta) \tag{5}$$

Given three equations and three unknowns, (1) can be rearranged in the following form:

$$r = \frac{k_1 y}{u\cos(\theta)} \tag{6}$$

Due to the complex nature of the non-linear tire model, deriving an equation for the vehicle's yaw rate as a function of steering angle would have proved extremely difficult. Instead, an iterative tuning approach was taken to estimate the relationship. Several iterations of simulations were run using various desired yaw rates across a range of vehicle speeds. Through the comparison between the actual and desired yaw rates of the vehicle, the following relationship was derived:

$$\frac{r}{\delta} = \frac{-7.07\times10^{-4}u^2 - 9.78\times10^{-3}u + 1.89}{1.6} \tag{7}$$

This relationship was then substituted into the controller to yield robust steering control over the multi-body model at a desired yaw rate.

C. Maneuver Set-up

In this study, there were two primary modes of failure: a lack of stability resulting from an overly aggressive maneuver, or insufficient maximum achievable yaw rate (excessive overshoot). To circumvent the latter, the vehicle should not affect traffic in lanes other than it's initial and final lane. Given that a standard lane in Ontario has a width of three metres per [10], an maximum overshoot of 1.5 m (half of a standard lane) was deemed acceptable. To address the issue of vehicle instability, the system must remain controllable for the entire duration of the maneuver.

Because a vehicle must have forward velocity to turn, a vehicle's yaw dynamics are tied to its forward speed. At higher speeds, the tire deflects more under cornering allowing for higher yaw rates to be achieved. As the vehicle continues to approach its maximum yaw rate however, the vehicle becomes less stable and is more likely to lose control. On the contrary, it is much more difficult for a vehicle to achieve the same tire deflections at lower speeds. This implies that the vehicle becomes significantly more stable at the cost of maximum yaw rate. Using empirical data from the simulated yaw rate and body slip angle data, a relationship between the vehicle's maximum yaw rate and forward speed was estimated. To ensure maximum performance from the tires, the estimated yaw rate was further incremented until vehicle stability was impacted during the maneuver.

Beginning with maximum braking force, the vehicle was required to brake down from an initial speed of 30 m/s (108 kph) to the desired final speed before turning at the vehicle limits. In subsequent tests, the braking force was then limited to a lower value to allow the vehicle to turn while braking. Because braking offers the vehicle additional time until collision, maneuver time was not a strong metric of vehicle performance. Instead, the forward distance travelled while the vehicle was in its initial lane was used to evaluate and compare the performance of the vehicle between experiments.

III. RESULTS

To begin, a no-brake strategy was used to evaluate the effectiveness of introducing braking. Travelling at 30 m/s, the model was able to successfully change lanes in a minimum distance of 29.5 metres while maintaining a constant speed. For reference, the vehicle managed to achieve a maximum lateral acceleration of 0.9 g and a peak yaw rate of 0.5 rad/s. Following this test, a brake-first strategy was employed. Under this strategy, the vehicle would utilize the full capabilities of the tires allowing it to slow as quickly as possible. Subsequent to the initial braking action, the vehicle would be able avoid at a lower speed allowing it to corner better than the benchmark no-brake strategy. To better visualize the control strategy, an image of the vehicle's traction circle has been provided in Figure 2. For this strategy, the vehicle's operating point lies at the bottom of the circle until the vehicle has reached its final desired speed. The vehicle then transitions to the horizontal axis where it may operate anywhere along the horizontal red line to complete the maneuver.

To test other locations around the traction circle, some mixed braking and steering strategies were analyzed. Instead of utilizing the full capabilities of the tires while braking, the brake force was limited to approximately 86% of the force applied in the brake-first strategy. By restricting the braking strength, the vehicle was able to use the remaining force to corner while braking. To represent this graphically, the operating point of the vehicle was confined to the green dotted line in Figure 2 while braking. Once the desired final speed was achieved, constant speed was maintained and the vehicle was free to operate along the horizontal axis for the rest of the maneuver.

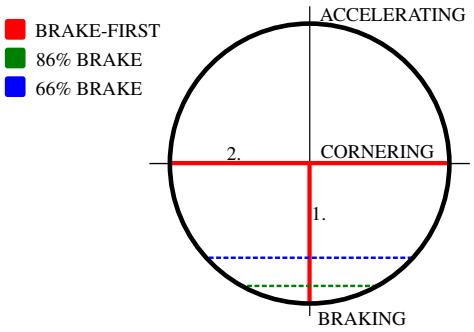

Figure. 2. A depiction of the vehicle's operating points along its traction circle during different braking strategies.

While braking, the maximum yaw rate of the vehicle would be limited. A restriction was therefore placed on the steering controller's output to maintain stability during this time. To find this limit, an iterative process similar to the one used for finding the vehicle's limits in the brake-first maneuver was followed. In order to establish a trend, another study was performed using this strategy with braking force limited to 66% of the vehicle's full braking capability.

A. *Maneuver Distance - Brake-First Strategy*

When braking within 2 m/s of the vehicle's initial speed, little to no reduction in maneuver distance was observed. Beyond approximately 28 m/s however, the maneuver distance began to grow at an approximate rate of 1 $\frac{\text{m}}{\text{m/s}}$. As braking was held constant until the desired maneuver speed was achieved, the braking distance grew linearly as the desired maneuver speed fell.

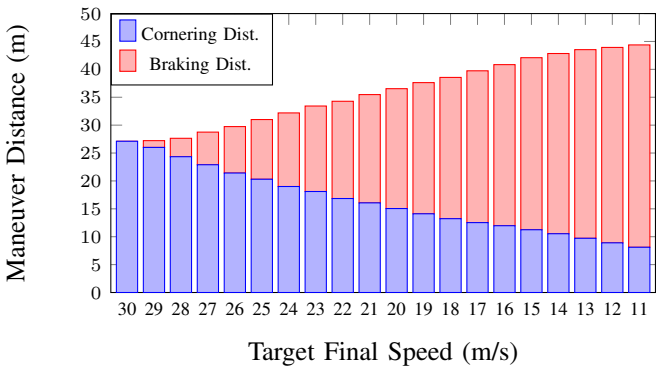

Figure. 3. A plot of the forward distance required to complete the maneuver at various desired final speeds under the full-brake strategy. The data is broken down into both the distance spent braking (red) and the distance spent evading (blue).

Unlike the braking distance, the distance travelled while cornering decreased with diminishing returns as the maneuver speed was reduced (shown by the decreasing size of the blue bars in Figure 3). Shown in Figure 4, the vehicle's maximum yaw rate grew as its maneuver speed fell. With a higher yaw rate, the vehicle was able to rotate quicker and follow a more aggressive path. Interestingly, despite a plateau at a maximum yaw rate of 2.2 rad/s after 15 m/s, the vehicle's maneuver distance continued to fall. It was found that as the vehicle slowed, the time spent cornering at the maximum yaw rate increased while the vehicle travelled forward at a slower pace. As a result of more time spent at its maximum yaw rate, the vehicle was able to achieve a larger change in heading angle to follow a slightly more aggressive path.

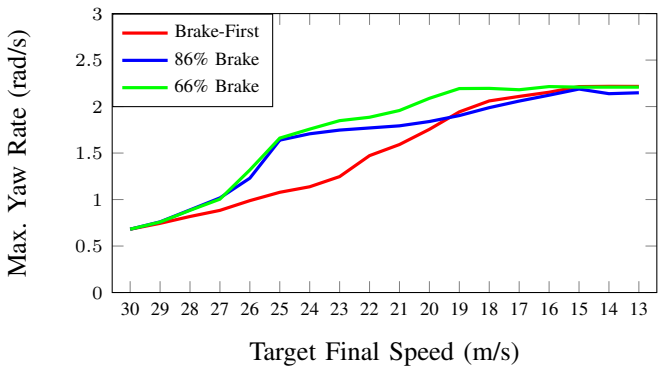

Figure. 4. A plot of the vehicle's maximum yaw rate versus maneuver speed under the different braking strategies.

Despite the benefits of reducing the maneuver speed, the increase in vehicle maneuverability was insufficient to offset the additional braking distance. As the maneuver distance was unable to be meaningfully reduced relative to the benchmark no-brake strategy, braking first to maximize vehicle handling was found to be a poor evasive strategy.

B. *Maneuver Distance - Combined Strategy*

Unlike the previous maneuver, when using a combined braking and steering strategy, the entirety of the vehicle's grip was not consumed by braking (implying the vehicle could begin its maneuver during the braking period). By combining the two-step maneuver into a single action, the simulations showed a dramatic decrease in distance required to complete the maneuver.

Although it was found that the performance of the vehicle rose with a reduction in braking strength, diminishing returns were present. These diminishing returns were potentially the result of the transitions between studied operating points along the traction curve. As the brake-first and 86% strategy resulted in desired operating points along the bottom of the traction circle (see Figure 2), a small decrease in braking strength yielded a large increase in available cornering force. As the braking strength continued to decrease (as in the 66% braking strategy), the desired operating point of the vehicle shifted to a more vertical position along the traction circle. Therefore, one would expect to see continued diminishing returns as the sensitivity in cornering force decreases around the traction circle. This trend is demonstrated in Figure 5, as the vehicle's maneuver distance decreased with braking strength.

Unlike the comparison with the brake-first strategy, it was found that the performance of the combined strategies were almost identical within 5 m/s of the initial speed. To explain

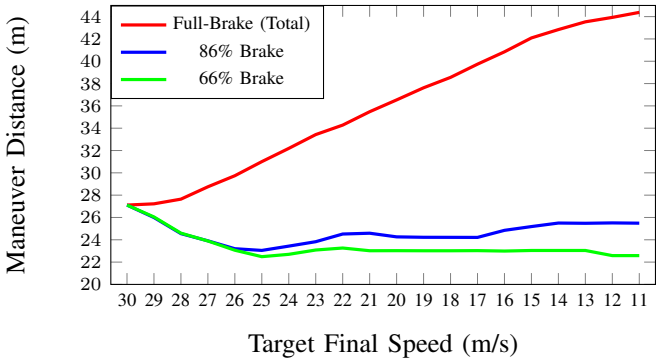

Figure. 5. A plot of the forward distance required to complete the maneuver under different braking strategies at various desired final speeds.

this behaviour, it is important to understand that the vehicle was not always operating at its limits throughout the entirety of the maneuver. During the initial evasive action and overshoots, the desired path was achieved at the limits of the vehicle. Before each overshoot however, significantly less yaw motion was required as the vehicle transitions between turning left and right. Until a final speed of 26 m/s, most of the braking occurred between overshoots (shown in Figure 6). As a result, the system was able to comfortably remain along its desired path while braking without encroaching on the vehicle's limits. This behaviour resulted in similar operating points under both strategies and thus a region of insensitivity to braking strength above 26 m/s.

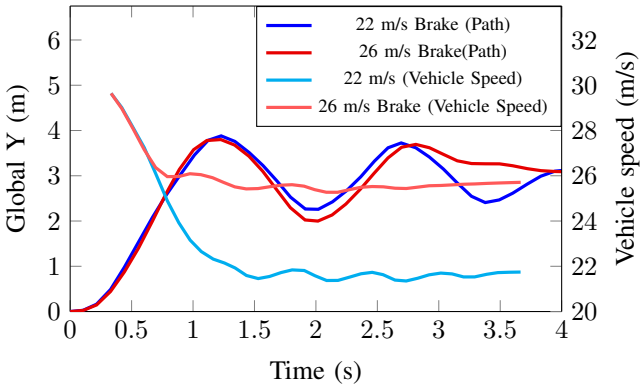

Figure. 6. A plot of the path travelled by the vehicle versus time overlaid with the vehicle speed throughout the maneuver.

Upon comparison of the maximum yaw rates between combined strategies, the vehicle was able to achieve higher yaw rates under lesser braking. Although this was the case under mixed-braking strategies, the vehicle was unable to achieve the same yaw rates under the brake-first strategy. While many factors affect a vehicle's handling, it is conceivable how a vehicle's handling may improve under braking. As the vehicle limits are related to the normal forces acting on the tires, the total force available at the front tires would have increased as weight was transferred forward under braking.

Further analyzing the yaw rates of the vehicle, more insight regarding the optimal path of the vehicle was attained. To evade more rapidly, the vehicle was permitted to overshoot its desired setpoint. However, as the vehicle overshoots, the radius required to reorient the vehicle is tighter than the original maneuver. Once a final desired speed of 26 m/s was reached, the vehicle's braking point encroached on the 'recovery' portion of the maneuver (where the vehicle must reorient itself with its new lane). As the vehicle progresses, its required yaw rate rises rapidly while the vehicle continues to brake. As the vehicle began braking into its first overshoot, the difference in the available cornering force between mixed braking strategies resulted in a difference between maneuver distances. From final speeds of 26 m/s to 25 m/s, braking into the first overshoot resulted in a maximum difference of approximately 0.5 metres between combined braking strategies. As the desired final speed continued to fall beyond 25 m/s, this braking continued further into the initial overshoot causing the maneuver distance to rise. One area of particular interest in Figure 5 is near 22 m/s. Here, the simulated data shows a 'hump' under both combined strategies. At this desired final speed, the vehicle ceases braking around the apex of the first overshoot – where the vehicle's maximum yaw rate is achieved (demonstrated in Figure 7). These humps were predicted to be the result of the rapid transition between brake-limited and stability-limited steering control.

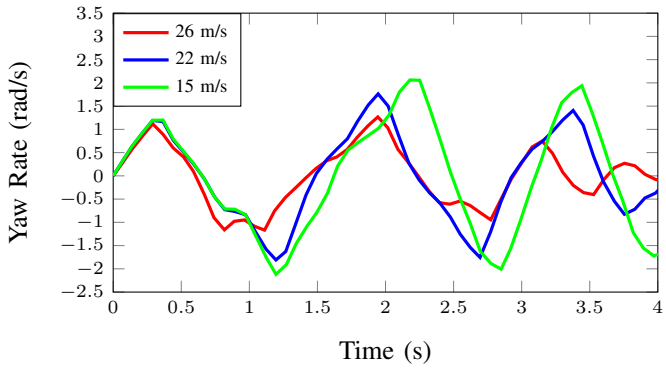

Figure. 7. A plot of vehicle's yaw rate throughout the maneuver.

As the vehicle continued to achieve lower final speeds, it continued to brake through more overshoots as it converged to its desired setpoint. In order to compensate for the reduction in available cornering force, the vehicle was required to take a less aggressive path to its goal. The effects of the path relaxation are visible in Figure 5 as the maneuver distance rises beyond 25 m/s under both strategies. Interestingly, the result of the new optimal path taken by the vehicle is a delay in the location at which the maximum yaw rate is achieved. At higher speeds, the vehicle's maximum yaw rate was achieved in the initial evasive action. As the vehicle approaches 25 m/s, the maximum yaw rate shifts towards the peak of the first overshoot. This pattern continues as the maximum yaw rate is achieved at later overshoots at slower final speeds. Shown in Figure 7, the system's settling time is greatly increased as a result.

Finally, as the vehicle's desired maneuver speed slowed beyond 15 m/s, the vehicle's response was unaffected by further braking. At these speeds, the vehicle was unable to reach its target final speed before the end of the maneuver. As a result, any additional braking beyond this point did not contribute to the vehicle's handling during the maneuver.

IV. CONCLUSIONS

Through experimentation with different braking strategies, several patterns emerged. Perhaps most notably, a brake-first strategy was found to be unsuitable for collision avoidance at highway speeds. Using a brake-first strategy, the vehicle suffered as the longer braking distance outweighed the benefits of improved cornering performance. On the contrary, braking was shown to be an effective addition to an evasive maneuver when implemented in a single action with cornering. By combining both actions into a single maneuver, the effects of the additional braking distance were muted. Additionally, it was found that the effectiveness of the braking was discovered to be inversely tied to the braking strength. As the vehicle's operating point moved around the traction circle however, its sensitivity to changes in braking strength diminished. Despite this, a comparison between studies showed that the choice of braking strength played a more significant role than braking distance in the effectiveness of the maneuver. Finally, under both combined strategies, an optimal braking distance appeared around 25 m/s before a loss in performance. This improvement was predicted to be the result of the vehicle achieving its final desired speed before the first overshoot. Despite these findings however, the data presented within this paper is only sufficient for the estimation of trends. As such, more studies need to be conducted to affirm these hypotheses and test the sensitivity of the results against different vehicle parameters.

REFERENCES

[1] C. Smith, *Tune to Win*. 1978, pp. 24–25.

[2] B.P.Minaker, *Equations of motion library for julia*, Accessible via: https://github.com/BPMinaker, 2023.

[3] E. Kuiper and J. J. M. V. Oosten, "The PAC2002 advanced handling tire model," *Vehicle System Dynamics*, vol. 45, no. 1, pp. 153–167, 2007.

[4] C. Samak, T. Samak, and S. Kandhasamy, "Control strategies for autonomous vehicles," *Autonomous Driving and Advanced Driver-Assistance Systems (ADAS): Applications, Development, Legal Issues, and Testing*, vol. 1, pp. 34–84, 2021.

[5] Y. Zhang, Y. Qin, M. Dong, T. Xu, and E. Hashemi, "Multi-objective predictive control for intelligent vehicles by considering stability constraints in complex scenarios," pp. 1–10, 2023, Date Accessed: Sept 2023.

[6] J. Yu and L. Petnga, "Space-based collision avoidance framework for autonomous vehicles," *Complex Adaptive Systems Conference with Theme: Cyber Physical Systems and Deep Learning*, vol. 140, pp. 37–45, 2018.

[7] B. Alrifaee, K. Jostyszyn, and D. Abel, "Model predictive control for collision avoidance of networked vehicles using Lagrangian relaxation," *IFAC-PapersOnline*, vol. 49, no. 3, pp. 429–435, 2016, Date Accessed: Oct 2023.

[8] Z. Sun, J. Zou, G. Xu, D. He, and W. Zhu, "Collision-avoidance steering control for autonomous vehicles using fast non-singular terminal sliding mode," *CAA International Conference on Vehicular Control*, pp. 1–6, 2020, Date Accessed: Oct 2023.

[9] A. da Silva Junior, C. Birkner, R. N. Jazar, and H. Marzbani, "Vehicle later dynamics with sliding mode control strategy for evasive maneuvering," in *Proceedings of the 2021 9th International Conference on System and Control*, 2021, pp. 165–172.

[10] *Road engineering design guidlines*, City of Toronto, Accessible via: https://www.toronto.ca/wp-content/uploads/2017/11/, Accessed Nov 15, 2023, 2017.